

# Characterization of an ASIC for CPG Sensors With Grid-Only Depth of Interaction Sensing

Gianluigi De Geronimo, Aleksey E. Bolotnikov, Gabriella Carini, Jack Fried, Paul O'Connor, and Stephen A. Soldner

**Abstract**—A new version of the front-end application specific integrated circuit (ASIC) for co-planar-grid (CPG) sensors is presented. Compared to the first version, the ASIC is optimized for signal/noise performance, modified in peaking time, and it implements timing signals to measure the depth of interaction using the grids signals only. Experimental results using state-of-the-art CPG sensors and different approaches for reducing the error due to electron trapping are reported. A new technique that makes use of the sum and difference of the grids signals is also presented.

**Index Terms**—Application specific integrated circuit (ASIC), co-planar-grid (CPG), CZT.

## I. INTRODUCTION

THE co-planar-grid (CPG) sensor is a compact and efficient solution for making large-volume room-temperature Gamma-ray spectrometers. It is being considered in applications ranging from nuclear material safeguard to radioisotope identification in security and defense, environmental remediation, well logging, medical diagnostics, and gamma-ray astronomy [1]–[4]. The availability of an application specific integrated circuit (ASIC) for CPG sensors is beneficial, especially in view of portable and battery operated detection systems.

By subtracting the signals from two co-planar grids, the CPG is sensitive to electrons only, overcoming the limit of poor holes mobility. The electron trapping is typically compensated either with the relative gain technique [5] or by measuring the depth of interaction through the cathode signals [6].

The ASIC here reported provides amplification of grids, difference and cathode signals, adjustable relative gain, high-order filtering with output baseline stabilization, and timing signals. It allows measurement of all signals of interest and electron trapping compensation using both techniques. A first version of the ASIC was presented in [7]. The new version presented here differs with respect to the previous in three aspects. First, the front end is optimized for resolution making use of the noise analysis results from the previous work. Second, the peaking time, originally 5  $\mu\text{s}$ , is now adjustable between 1.2  $\mu\text{s}$  and 2.4  $\mu\text{s}$ . Third,

grids only timing signals allow compensation for the electron trapping without cathode signal [7]. As in the previous version, the ASIC was fabricated in CMOS 0.25  $\mu\text{m}$  technology and, with an area of about 9.5  $\text{mm}^2$ , it dissipates about 25 mW.

In this summary Section II describes the new architecture with some details on the front-end optimization, and Section III reports some experimental results. In Section IV a new technique is proposed for the measurement of the depth of interaction through the amplitude of the grids sum and difference signals only.

## II. ASIC ARCHITECTURE AND CHARACTERIZATION

In Fig. 1, the block diagram of the ASIC architecture is shown. It implements three front-end channels, two for the grids signals and one for the cathode signal. This architecture, which may appear very similar to the one reported in [7], implements three major changes.

The first improvement consists of a redesign of the front-end stages by replacing the n-channel input device with a p-channel device. The noise analysis and experimental results in [7] demonstrated that, due to the correlation associated with the intergrid capacitance, the series input noise from the front end can severely limit the resolution of the system. The series noise, dominated by the low-frequency component, can be appreciably reduced if a p-channel device is used [8]. This change also required a rearrangement of the dual-stage charge gain configurations, by appropriately inverting the two stages [7].

The second improvement consists of decreasing the peaking time from the original 5  $\mu\text{s}$  value, having it selectable between 1.2  $\mu\text{s}$  and 2.4  $\mu\text{s}$ . This change makes the ASIC suitable for use with larger CPG sensors, typically characterized by higher leakage currents. In Fig. 2, the measured equivalent noise charge (ENC) versus the peaking time for different values of the relative gain  $G$  are shown. For comparison, the measurement from the previous ASIC version is also reported [7]. The measurement was made by using the ASIC output from the first real pole of the shaper, followed by a suitable combination of differentiation and integration with the Ortec 450 research amplifier. The increase in parallel noise observed at longer peaking times is partially due to the noise contribution from the real pole stage of the shaper in the ASIC (set at 360 ns and optimized for the 1.2  $\mu\text{s}$  peaking time) and partially due to the different noise weighting function (lower order [8]). The improvement in resolution at the peaking times of interest (1.2  $\mu\text{s}$  and 2.4  $\mu\text{s}$ ) can be observed. For values of relative gain  $G \approx 1$  the full-width at half-maximum (FWHM) for this sensor is reduced from 11.5 keV to

Manuscript received November 11, 2005; revised January 15, 2006.

G. De Geronimo, J. Fried, and P. O'Connor are with the Instrumentation Division, Brookhaven National Laboratory, Upton, NY 11973 USA.

A. E. Bolotnikov is with the Nonproliferation and National Security Department, Brookhaven National Laboratory, Upton, NY 11973 USA.

G. Carini is with the Energy, Environment and National Security Directorate, Brookhaven National Laboratory, Upton, NY 11973 USA, and also with the Department of Electrical Engineering, University of Palermo, Palermo 90100, Italy.

S. A. Soldner is with the eV Products, Division of II-VI, Inc., Saxonburg, PA 16056 USA.

Digital Object Identifier 10.1109/TNS.2006.871260

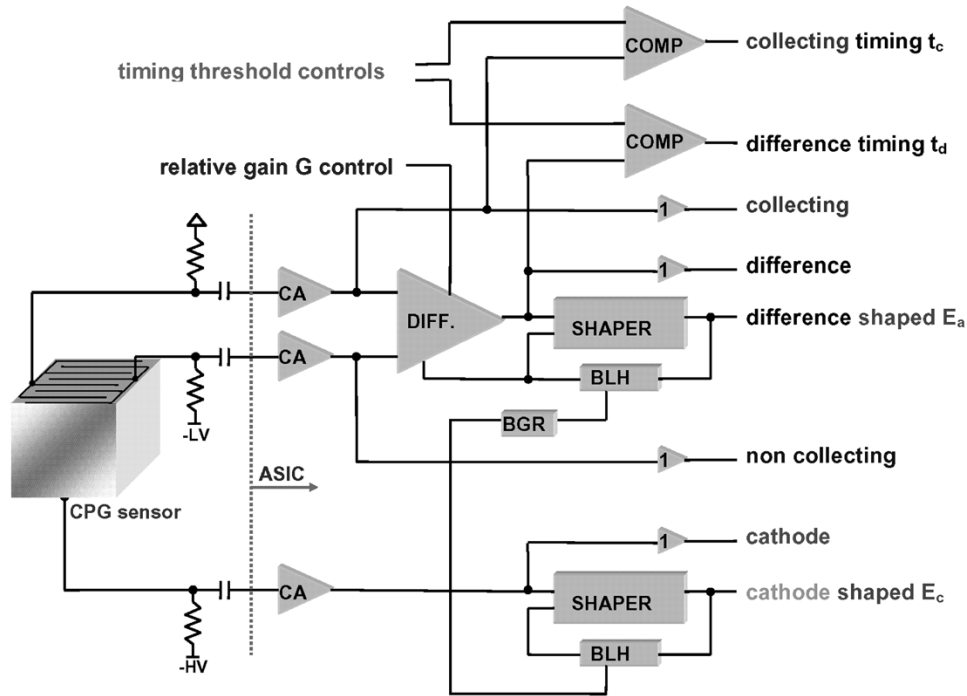


Fig. 1. Block diagram illustrating the ASIC architecture.

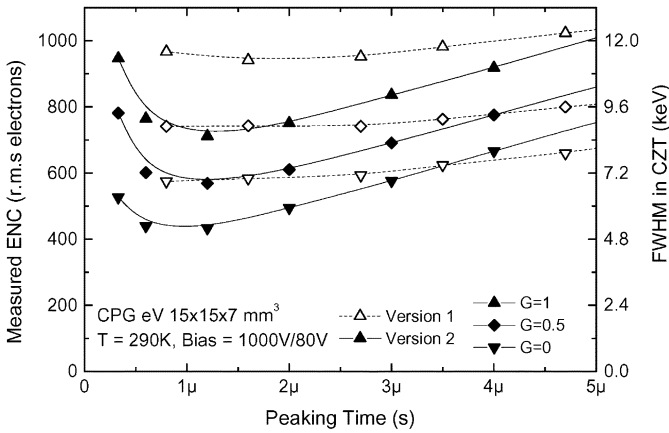


Fig. 2. Measured ENC versus peaking time for different values of the relative gain  $G$  with the CPG sensor connected and biased (solid symbols). The results from the old version are also reported for comparison (open symbols).

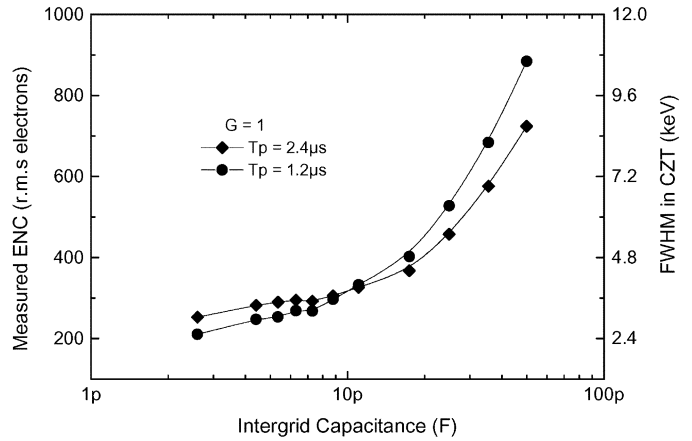


Fig. 3. Measured ENC versus intergrid capacitance for relative gain  $G = 1$  and the two values of peaking time.

8.4 keV, corresponding to about a factor 2 in power. In Fig. 3, the measured ENC of the ASIC versus the intergrid capacitance for relative gain  $G = 1$  and the two values of peaking time is shown.

The third improvement consists of measuring the timing of the collecting signal in place of the one of the cathode signal. The timing delay  $\Delta t = t_d - t_c$  from the collecting signal to the difference signal is a measure of the depth of interaction (see Fig. 4). The error due to the threshold, positioned a value  $V_{th}$  above the baseline of the signal, can be corrected with  $\Delta t_{eff} \approx \Delta t + 0.5 \Delta t_{max} V_{th} / E_d$ , where  $\Delta t_{max}$  is the maximum transit time for the electrons,  $E_d$  is the amplitude of the difference signal for the specific event, and 0.5 takes into account the partial induction due to a single grid. The depth of interaction  $d$

can be calculated as  $d \approx d_{max} \Delta t_{eff} / \Delta t_{max}$ . This concept, already introduced in [7], allows the measurement of the depth of interaction by using the grids signals only (collecting and difference). The biparametric data (energy  $E_d$  and depth  $d$  for each event) can be used to correct for the electron trapping.

This technique has some advantages compared to the two known techniques. With respect to the relative gain approach, it does not require hardware adjustments to adapt the compensation and can be applied either in real time or after the acquisition. With respect to the cathode/difference ratio correction technique, it does not require the additional cathode amplification and processing with advantages in terms of power and area, especially considering the need for bulky capacitors for the coupling of the high-voltage cathode to the ASIC.

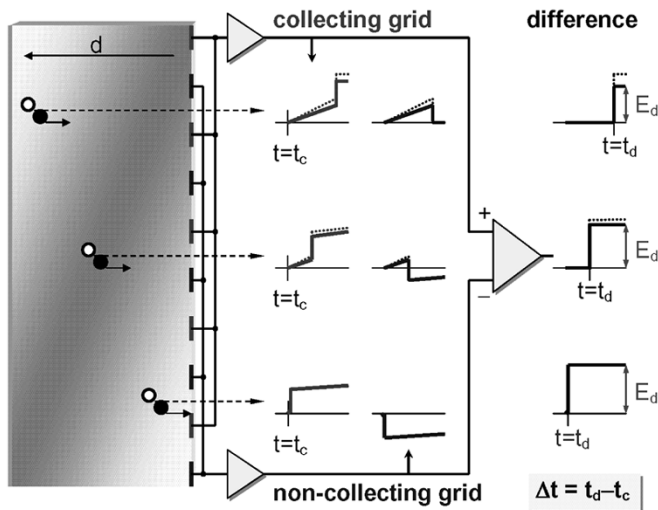


Fig. 4. Schematic of the concept of measuring the depth of interaction from the timing delay  $\Delta t$  between the collecting signal timing  $t_c$  and the difference signal timing  $t_d$ .

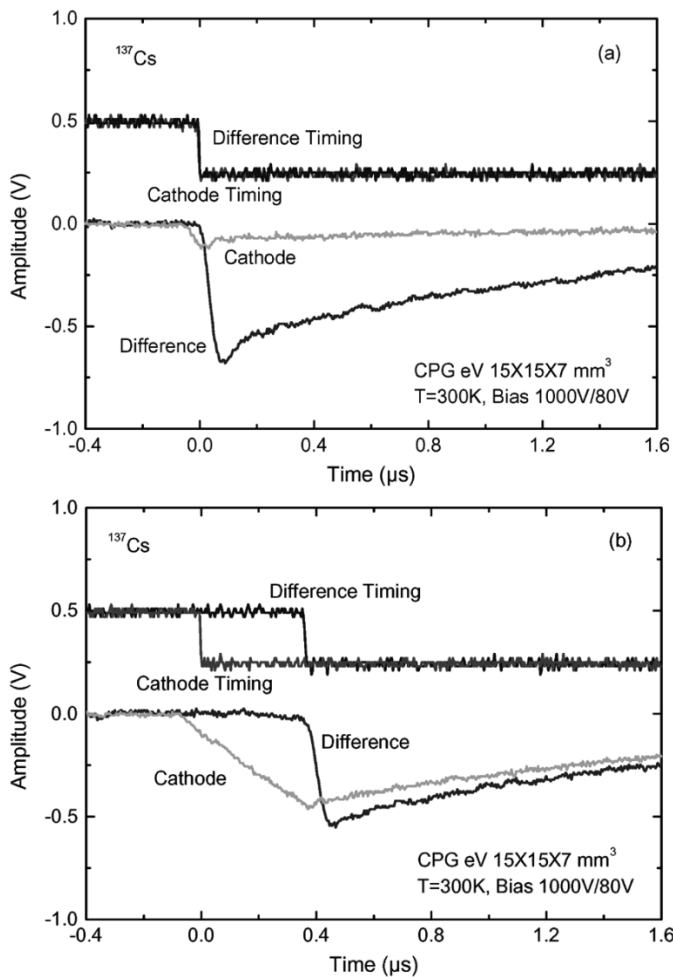


Fig. 5. Measured unshaped and timing responses from the ASIC-CPG system to  $^{137}\text{Cs}$  signals for an interaction (a) close to grid and (b) close to cathode.

Shown in Fig. 5 are the unshaped and timing responses of the ASIC-CPG system to  $^{137}\text{Cs}$  signals for a) an interaction close to grid where the timing delay is small and b) an interaction close

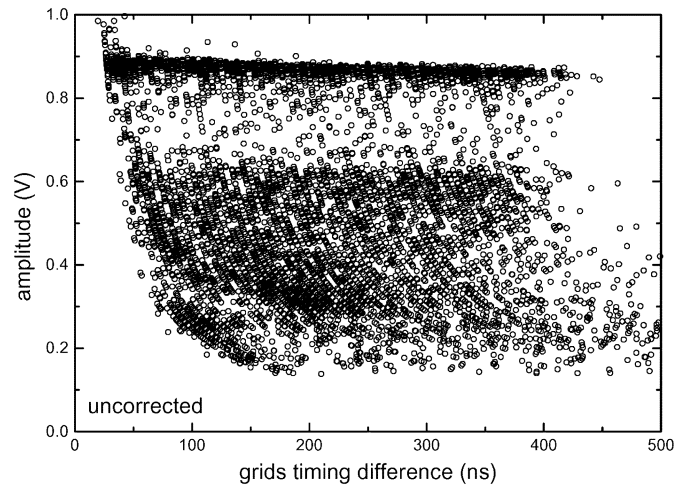


Fig. 6. Biparametric spectrum from  $^{137}\text{Cs}$  measured using the grids timing difference, which is directly related to the depth of interaction.

to the cathode where the timing delay is large. In Fig. 6, the biparametric spectrum (energy  $E_d$  versus depth  $d$  for each event) from  $^{137}\text{Cs}$  signals, corrected for the error due to the threshold, is shown. In this measurement, the relative gain  $G$  was set to 1, and the trapping effect on the 662 keV line (amplitude average decreasing from 0.89 V to 0.86 V from grids to cathode) can be observed. The correction for electron trapping depends on the depth of interaction and, once extracted from this measurement, it can be applied to following measurements on each event in real time. If a linear correction is used, a result comparable to the relative gain compensation technique should be expected.

### III. SPECTRAL MEASUREMENTS

The ASIC-CPG system was characterized using the relative gain compensation technique and the depth of interaction correction technique. In the first case, the measurements were done at eV Products using state-of-the-art CPG sensors. In the second case, the measurements were done in Brookhaven National Laboratory, Upton, NY, with the same sensors used to characterize the previous version of the ASIC, and the acquisition chain included the peak detector derandomizer (PDD) ASIC [9], a custom acquisition board and LabView<sup>1</sup> environment.

#### A. Relative Gain Compensation Technique

All measurements reported here were done at temperature  $T \approx 23^\circ\text{C}$  and using sources without collimator. In Fig. 7, the spectra from (a)  $^{57}\text{Co}$  and  $^{137}\text{Cs}$ , (b)  $^{22}\text{Na}$ , and (c)  $^{60}\text{Co}$  are shown with a  $1\text{ cm} \times 1\text{ cm} \times 1\text{ cm}$  CPG sensor.

In Fig. 8, the spectrum from a  $^{137}\text{Cs}$  source with a  $1.5\text{ cm} \times 1.5\text{ cm} \times 1.5\text{ cm}$  CPG sensor is shown. The ASIC-CPG system was also tested for high rate. In Fig. 9, the spectra from a  $^{133}\text{Ba}$  source with a  $1\text{ cm} \times 1\text{ cm} \times 0.75\text{ cm}$  CPG sensor at 1 kcps (kilo counts per second) and 70 kcps

<sup>1</sup><http://www.labview.com/>

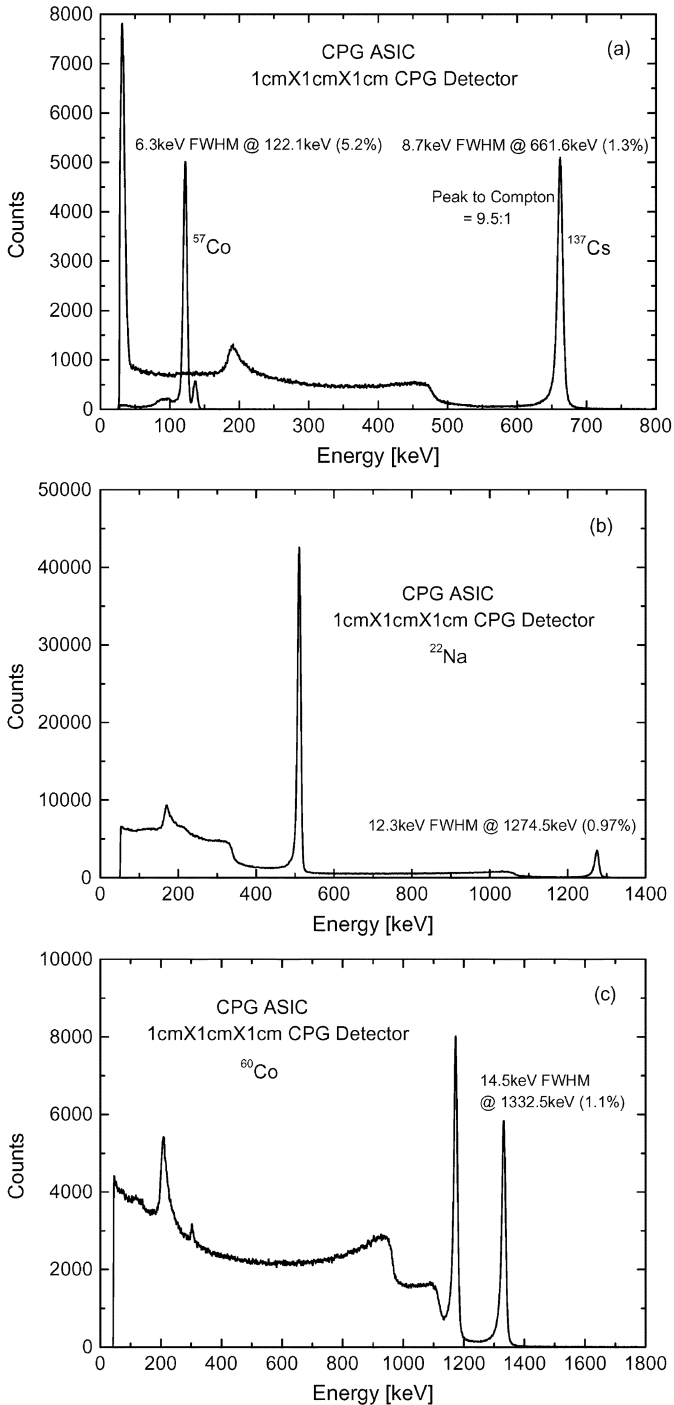


Fig. 7. Spectral measurements from (a)  $^{57}\text{Co}$  and  $^{137}\text{Cs}$ , (b)  $^{22}\text{Na}$ , and (c)  $^{60}\text{Co}$  sources with a 1 mm  $\times$  1 mm  $\times$  1 mm CPG sensor.

rates are shown. Some deterioration of the spectrum due to the pile-up is observed.

### B. Depth of Interaction Correction Technique

All measurements reported here were done at temperature  $T \approx 27^\circ\text{C}$  and using a  $^{137}\text{Cs}$  source without collimator. In Fig. 10, measurements using the cathode/difference ratio are shown. The depth of interaction was calculated from a simple

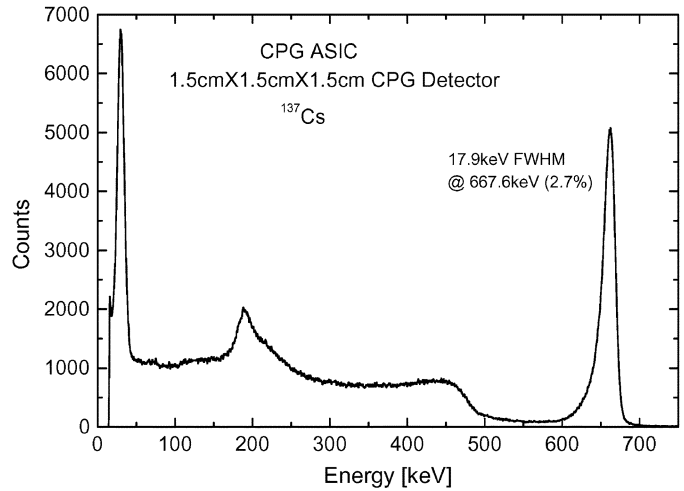


Fig. 8. Spectral measurements from a  $^{137}\text{Cs}$  source with a 1.5 cm  $\times$  1.5 cm  $\times$  1.5 cm CPG sensor.

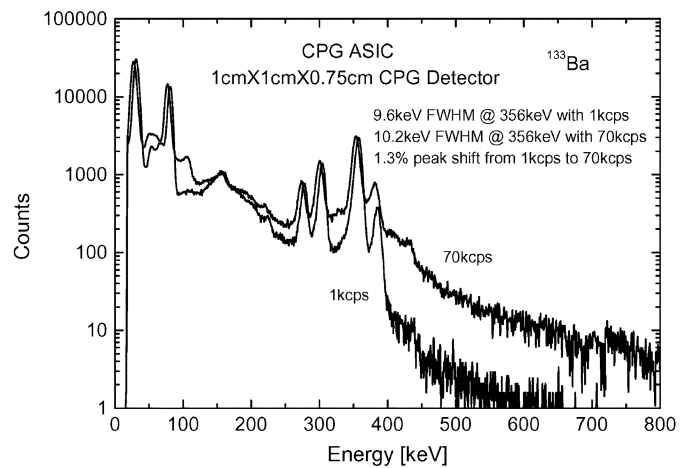


Fig. 9. Spectral measurements from a  $^{133}\text{Ba}$  source with a 1 cm  $\times$  1 cm  $\times$  0.75 cm CPG sensor.

linear approximation, and the second-order errors described in [10] were not included. The gain coefficient for the correction was calculated from the position of the 662 keV peak at each depth.

In Fig. 11, corresponding measurements using the grids timing difference are shown. The difference at low energy between the spectra at different depths in both techniques is partially due to threshold effects and result in some low-energy events attributed to a wrong depth. Further investigation of these aspects is needed. However, since the cumulative spectrum is eventually used, the impact on the overall process is small. In Fig. 11(b), the spectrum where the first two data sets from the grids were removed is also shown, renormalized to the full corrected spectrum. In front of a  $\approx 15\%$  loss in counts, an improvement in the spectral performance on the right side of the 662 keV spectral line can be observed. The worsening of the spectral response at the right side of the 662 keV spectral line for event close to the grids was already observed and discussed in [6].

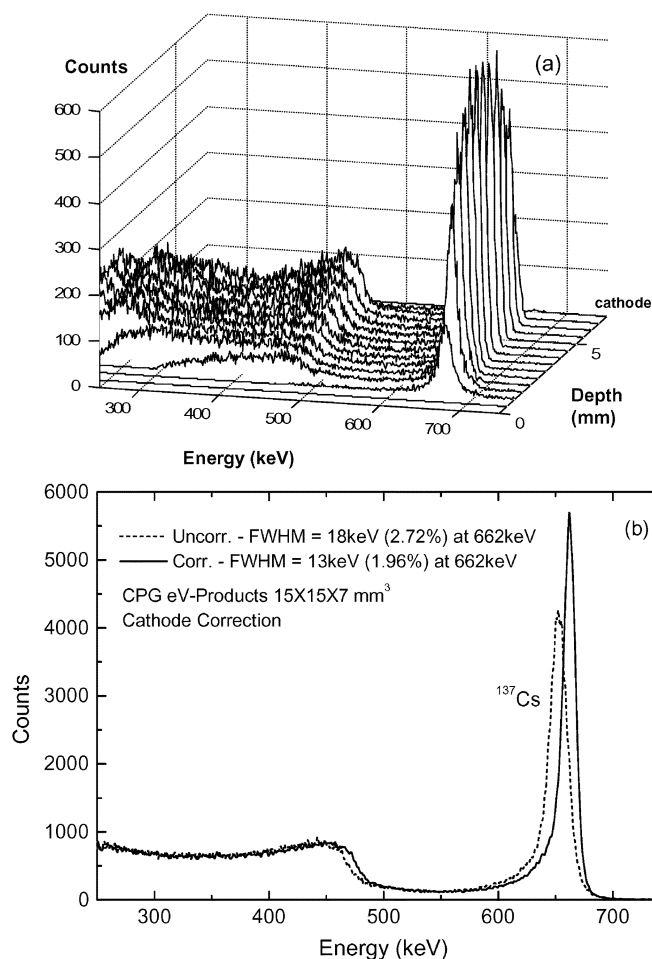


Fig. 10. Spectral measurements from a  $^{137}\text{Cs}$  source with a  $1.5\text{ cm} \times 1.5\text{ cm} \times 0.7\text{ cm}$  CPG sensor. The 662 keV peaks for the spectra at different depths in (a), calculated from the cathode/difference ratio, were used to correct the cumulative spectrum in (b) increasing the resolution from 18 keV (uncorrected) to 13 keV (corrected).

#### IV. SUM OF GRIDS SIGNALS FOR DEPTH CORRECTION

The sum of collecting and noncollecting signals is an alternative approach to grids-only measurement of the depth of interaction. As suggested in [11] and [12], the sum of the two signals is, to a first order, equal to the cathode signal (some differences may be observed for the presence of guard rings). A noise analysis similar to the one reported in [7] shows that noise on the sum of the two signals is not affected by the correlation due to the intergrid capacitance. Compared to the use of the noncollecting signal, the sum has also the advantage of strongly reducing the dependence of the response on the position of the event with respect to the strips. This dependence is relevant for events close to the grids. In Fig. 12, measurements using the sum/difference ratio are shown. The collecting and noncollecting signals from the ASIC were summed using the Ortec 433 A summing amplifier and shaped using the Ortec 450 research amplifier. A detector exhibiting worse spectral performance compared to the one used in previous measurements was used in this case. The depth of interaction was again calculated from a simple linear

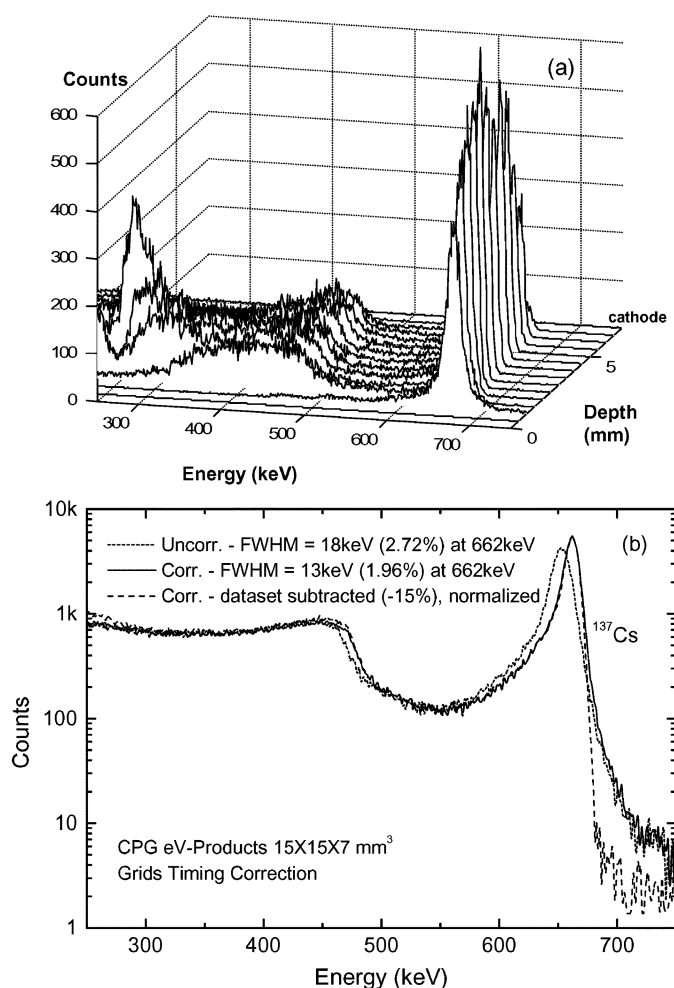


Fig. 11. Spectral measurements from a  $^{137}\text{Cs}$  source with a  $1.5\text{ cm} \times 1.5\text{ cm} \times 0.7\text{ cm}$  CPG sensor. The 662 keV peaks for the spectra at different depths in (a), calculated using the grids timing difference, were used to correct the cumulative spectra in (b) increasing the resolution from 18 keV (uncorrected) to 13 keV (corrected). The spectrum with two data sets removed and normalized is also shown.

approximation, and further investigation of second-order errors is needed. The correction process was carried out as in previous cases extracting the gain coefficient from the position of the 662 keV peak at each depth.

#### V. CONCLUSION

An application specific integrated circuit (ASIC) for co-planar-grid (CPG) sensors was presented. Compared to the previous version, this ASIC has improved electronics resolution and implements the signals for the measurement of the depth of interaction using grids signals only. The ASIC was characterized with CPG sensors, correcting for electron trapping using the relative gain compensation technique and the depth of interaction correction technique. The sum of the collecting and noncollecting signals is also proposed as alternative to the timing signals for a depth correction based on grids signals only.

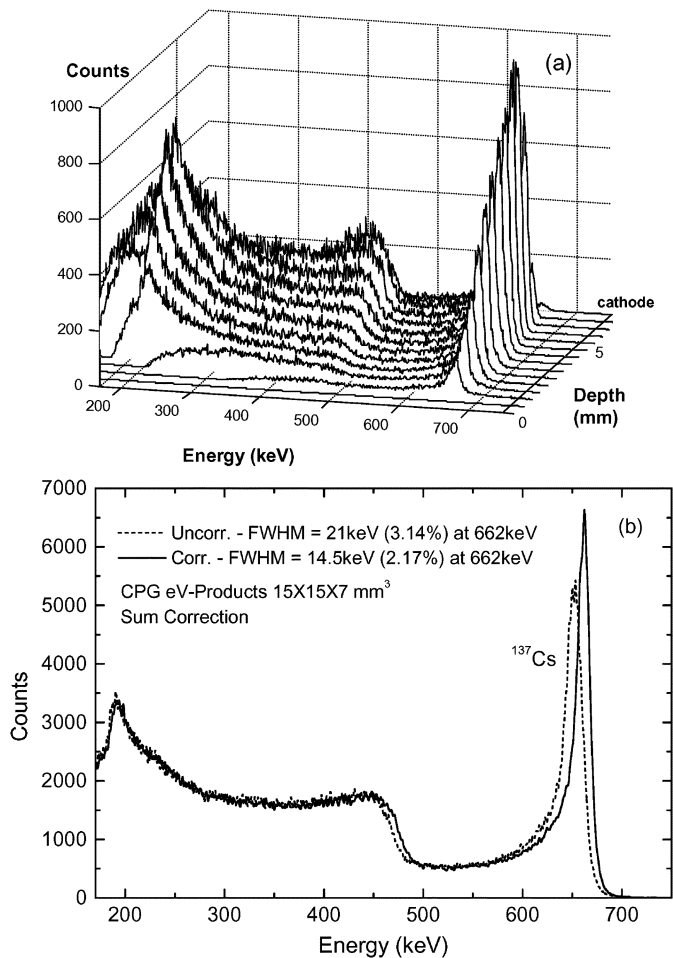


Fig. 12. Spectral measurements from a  $^{137}\text{Cs}$  source with a  $1.5\text{ cm} \times 1.5\text{ cm} \times 0.7\text{ cm}$  CPG sensor. The 662 keV peaks for the spectra at different depths in (a), calculated using the sum of collecting and noncollecting signals, were used to correct the cumulative spectra in (b) increasing the resolution from 21 keV (uncorrected) to 14.5 keV (corrected).

#### ACKNOWLEDGMENT

The authors from the Brookhaven National Laboratory, Upton, NY, are grateful to Dr. R. B. James for partially supporting their research in this field.

#### REFERENCES

- [1] R. Arlt, J. Brutscher, R. Gunnink, V. Ivanov, K. Parnham, S. A. Soldner, and J. Stein, "Use of CdZnTe detectors in hand-held and portable isotope identifiers to detect illicit trafficking of nuclear material and radioactive sources," *Proc. IEEE Nuclear Science Symp. (NSS) Conf. Board*, vol. 1, pp. 4/18–4/23, 2000.
- [2] T. H. Prettyman, K. D. Ianakiev, C. E. Moss, S. A. Soldner, M. R. Sweet, and M. C. Browne, "Developments of high efficiency, multi-element CdZnTe detectors for portable measurement applications," *J. Radioanal. Nucl. Chem.*, vol. 248, pp. 295–300, May 2001.
- [3] P. N. Luke, M. Amman, J. S. Lee, B. A. Ludewigt, and H. Yaver, "CdZnTe coplanar grid detector array for environmental remediation," *Nucl. Instrum. Methods Phys. Res. A*, vol. 458, pp. 319–324, 2001.
- [4] T. H. Prettyman, W. C. Feldman, K. R. Fuller, S. A. Storms, S. A. Soldner, C. Szeles, F. P. Ameduri, D. J. Lawrence, M. C. Browne, and C. E. Moss, "CdZnTe Gamma-ray spectrometer for orbital planetary missions," *IEEE Trans. Nucl. Sci.*, vol. 49, no. 4, pp. 1881–1886, Aug. 2002.
- [5] M. Amman and P. Luke, "Optimization criteria for coplanar-grid detectors," *IEEE Trans. Nucl. Sci.*, vol. 46, no. 3, pp. 205–212, Jun. 1999.
- [6] Z. He, G. F. Knoll, D. K. Wehe, R. Rojeski, C. H. Mastrangelo, M. Hamming, C. Berret, and A. Uritani, "Position-sensitive single carrier CdZnTe detectors," *Nucl. Instrum. Methods Phys. Res. A*, vol. 388, pp. 180–185, 1997.
- [7] G. De Geronimo, G. Carini, W. S. Murray, and P. O'Connor, "Front-end ASIC for co-planar grid sensors," *IEEE Trans. Nucl. Sci.*, vol. 52, no. 5, pp. 2003–2008, Oct. 2005.
- [8] G. De Geronimo and P. O'Connor, "MOSFET optimization in deep sub-micron technology for charge amplifiers," *IEEE Trans. Nucl. Sci.*, vol. 52, no. 6, pp. 3223–3232, Dec. 2005.
- [9] P. O'Connor, G. De Geronimo, and A. Kandasamy, "Amplitude and time measurement ASIC with analog derandomization: First results," *IEEE Trans. Nucl. Sci.*, vol. 50, no. 4, pp. 892–897, Aug. 2003.
- [10] W. Li, Z. He, G. F. Knoll, D. K. Wehe, and Y. F. Du, "A modeling method to calibrate the interaction depth in 3-D position sensitive CdZnTe gamma-ray spectrometers," *IEEE Trans. Nucl. Sci.*, vol. 47, no. 3, pp. 890–894, Jun. 2000.
- [11] A. E. Bolotnikov, G. S. Camarda, G. A. Carini, M. Fiederle, L. Li, G. W. Wright, and R. B. James, "Performance studies of CdZnTe detector by using a pulse shape analysis," *Proc. SPIE*, vol. 5922, pp. 220K1–220K12, 2005.
- [12] G. A. Carini, A. E. Bolotnikov, G. S. Camarda, G. De Geronimo, D. P. Siddons, G. W. Wright, and R. B. James, "New results from testing of coplanar-grid CdZnTe detectors," *Proc. SPIE*, vol. 5922, pp. 220M1–220M6, 2005.